ELSEVIER

Solid State Ionics 69 (1994) 59–67

SOLID STATE IONICS

Improved capacity retention in rechargeable 4 V lithium/lithium-manganese oxide (spinel) cells

R.J. Gummow, A. de Kock, M.M. Thackeray [1]

Division of Materials Science and Technology, CSIR, P.O. Box 395, Pretoria 0001, South Africa

Received 20 January 1994; accepted for publication 11 February 1994

Abstract

The rechargeable capacity of 4 V $Li_xMn_2O_4$ spinel cathodes ($0<x\leq 1$) has been improved by modifying the composition of the spinel electrode. Stable rechargeable capacities in excess of 100 mAh/g in flooded-electrolyte lithium cells can be achieved if $LiMn_2O_4$ is doped with mono- or multivalent cations (e.g. Li^+, Mg^{2+}, Zn^{2+}) or, alternatively, with additional oxygen to increase the average manganese-ion oxidation state marginally above 3.5.

1. Introduction

Over the past decade, the spinel $LiMn_2O_4$ has been studied extensively as an electrode for rechargeable lithium cells [1–7]. When $0\leq x\leq 1$, Li/$Li_xMn_2O_4$ cells discharge at 4 V versus lithium, whereas when $1<x\leq 2$, the cells discharge at 3 V. The 4 V electrode is significantly more stable to cycling than the 3 V electrode. At 4 V, the cubic symmetry of the Li_x-Mn_2O_4-spinel structure is maintained, which allows the electrode to expand and contract isotropically during lithium insertion/extraction reactions. When lithium is inserted into $Li_xMn_2O_4$ at 3 V, i.e. when the average manganese-ion valency falls below 3.5, a Jahn–Teller distortion is introduced into the spinel structure reducing the crystal symmetry from cubic to tetragonal. In $Li_xMn_2O_4$ ($1<x\leq 2$), the c/a ratio of the unit cell increases by 16%, which is too large for the electrode to maintain its structural integrity on cycling [1].

[1] Author to whom correspondence should be addressed at present address: Chemical Technology Division, Argonne National Laboratory, 9700 South Cass Avenue, Argonne, IL 60439, USA.

SSDI 0167-2738(94)00051-S

Although the 4 V $Li_xMn_2O_4$ electrode is significantly more stable to cycling than the 3 V electrode, a slow capacity fade has been encountered in the high-voltage range [4]. The capacity loss can be attributed to several possible factors:

(i) an instability of the organic-based electrolyte at the high voltages reached when charging cells,

(ii) a slow dissolution of the $Li_xMn_2O_4$ electrode into the electrolyte (as Mn^{2+}) according to the disproportionation reaction:

$$2Mn^{3+}\rightarrow Mn^{4+}+Mn^{2+},$$

(iii) the onset of the Jahn–Teller effect in deeply discharged $Li_xMn_2O_4$ electrodes (i.e. at $x\approx 1$).

Progress has already been made in the development of electrolytes that are stable above 4 V to combat point (i) above [5,8]. Several research groups have investigated the performance of manganese-substituted spinels $Li_xM_yMn_{2-y}O_4$ (M=Ti, Ge, Fe, Co, Zn, Ni) [7,9,10]. None of these substitutions lead to any significant increase in the cell capacity at 4 V nor to any significant decrease of the voltage drop at $x=1$. Substitution by cobalt was reported to combat

point (ii) [9]. We have attempted to combat point (iii) by specifically reducing the Mn^{3+}-ion concentration in the initial spinel electrode [11]. Three approaches were adopted to increase the average manganese-ion valency marginally above 3.5:

(a) synthesising stoichiometric spinels of general formula $Li_{1+\delta}Mn_{2-\delta}O_4$, i.e. by replacing some manganese with lithium. For example, when $\delta=0.05$ the spinel has the formula $Li_{1.05}Mn_{1.95}O_4$ in which $n^+_{Mn}=3.56$,

(b) replacing a small amount of manganese with a multivalent metal cation such as Mg^{2+} or Zn^{2+}. For example, when $\delta=0.025$ in $LiMg_{\delta/2}Mn_{2-\delta}O_4$, $n^+_{Mn}=3.54$ (note that this is a non-stoichiometric spinel with a slight cation deficiency),

(c) synthesising defect (cation-deficient) spinels $Li_{1-\delta}Mn_{2-2\delta}O_4$, for example, $Li_{0.975}Mn_{1.95}O_4$ ($\delta=0.025$) in which $n^+_{Mn}=3.60$.

The synthesis and electrochemical characterization of several spinel electrodes with modified composition are reported in this paper. The crystallographic parameters and cycling stability of these electrodes are compared with a standard $LiMn_2O_4$ electrode.

2. Experimental

Stoichiometric spinels with the general formula $Li_{1+\delta}Mn_{2-\delta}O_4$ with $\delta=0$ (i.e. standard $LiMn_2O_4$) and with $\delta=0.03$, 0.05, 0.10, 0.22 and 0.29 were synthesized by reacting the stoichiometric amounts of $LiOH\cdot H_2O$ and γ-MnO_2 (CMD) in air. Samples with $0\leq\delta\leq0.10$ were prefired at 450°C for 48 h and thereafter at 650°C for 48 h. Samples with $\delta=0.22$ and 0.29 were synthesized by firing once at 450°C for 96 h.

Samples doped with divalent cations M ($M=Mg^{2+}$, Zn^{2+}) with the general formula $LiM_{\delta/2}Mn_{2-\delta}O_4$ ($\delta=0.025$ and 0.05) were synthesized by reacting the required stoichiometric amounts of $LiOH\cdot H_2O$, γ-MnO_2 and $Mg(NO_3)_2\cdot 6H_2O$ or $Zn(NO_3)_2\cdot 2H_2O$ in air. Samples were initially preheated at 450°C for 48 h, reground and fired at 650°C for 48 h.

A defect spinel sample $Li_{1-\delta}Mn_{2-2\delta}O_4$ ($\delta\approx0.025$) was synthesized by reaction of $LiOH\cdot H_2O$ and γ-MnO_2 (Li:Mn = 1:2) in air, initially at 450°C for 48 h and then at 600°C for 48 h.

Unit-cell parameters of the spinel materials were obtained from powder X-ray diffraction data collected on an automated Rigaku diffractometer with Cu Kα radiation, monochromated by a graphite crystal. The lattice constants were determined by iterative least-squares refinements against an internal silicon standard. The lithium- and manganese contents in the final products were determined by atomic absorption spectroscopy.

The electrochemical characterization of the spinel samples was conducted in prismatic lithium cells with a flooded-electrolyte configuration at room temperature (22°C) [11]. A typical cathode mixture consisted of either the spinel, acetylene-black and an ethylene-propylene-diene-monomer binder (EPDM) in a 90:7:3 ratio by mass or, alternatively, of a mixture of 80% by mass of the spinel and 20% by mass of a 1:2 mixture of acetylene black and teflon (TAB). The cathode (20–30 mg) was pressed onto a stainless-steel mesh current collector, approximately 10 mm in diameter. The anode was lithium foil (Lithco), pressed onto a stainless-steel mesh. The electrolyte consisted of a solution of 1M $LiClO_4$ in anhydrous propylene carbonate (Aldrich), which was used as received. Anode and cathode were separated by a microporous polypropylene separator (Celgard 3401).

3. Results and discussion

Fig. 1a shows an isothermal slice of the ternary Li–Mn–O phase diagram that relates specifically to the positions of phases with spinel, defect-spinel and rock salt structures. An expanded view of the shaded section of the phase diagram is given in Fig. 1b. The region that contains the lithium-manganese-oxide spinel phases of particular interest is defined by the $LiMn_2O_4$–$Li_2Mn_4O_9$–$Li_4Mn_5O_{12}$ tie triangle. $Li_{1+\delta}Mn_{2-\delta}O_4$ compounds ($0\leq\delta\leq0.33$) that have the stoichiometric spinel composition AB_2O_4 are located on the tie-line between $LiMn_2O_4$ ($\delta=0$) and $Li_4Mn_5O_{12}$ ($\delta=0.33$). Defect-spinel phases that can be represented by the general formula $Li_{1-\delta}Mn_{2-2\delta}O_4$ ($0<\delta\leq0.11$) lie on the tie-line between $LiMn_2O_4$ and $Li_2Mn_4O_9$. Compounds that are marginally doped with excess lithium and in which the average manganese-ion oxidation state, n^+_{Mn}, lies between 3.5 and 3.63 are located within the shaded triangle, Li-

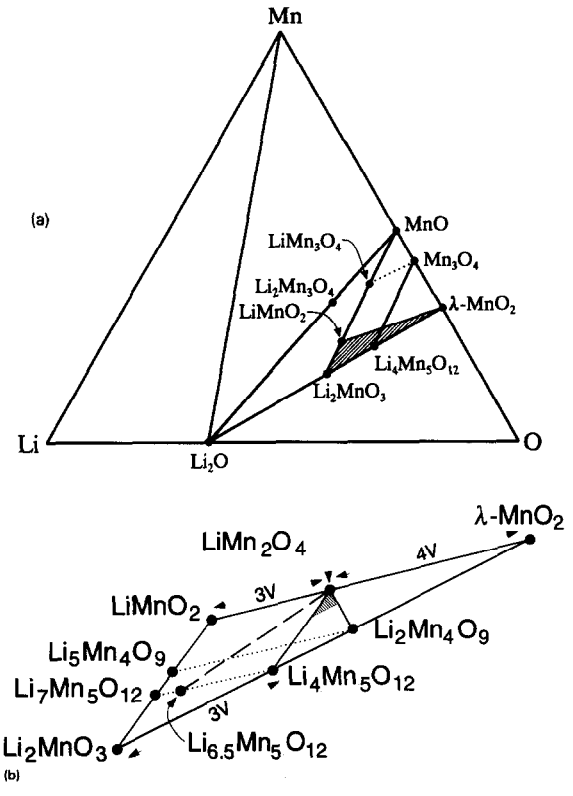

Fig. 1. (a) An isothermal slice of the ternary Li-Mn-O phase diagram at 25°C; (b) an expanded view of the shaded region of the phase diagram in (a).

Mn_2O_4–$Li_{1.10}Mn_{1.90}O_4$–$Li_{0.97}Mn_{1.94}O_4$ in Fig. 1b.

Lithium insertion into (and extraction from) the tetrahedral A-sites of the spinel structure occurs at 4 V versus lithium whereas insertion into/extraction from octahedral sites occurs at 3 V. Broadly speaking, the 4 V region lies within the $LiMn_2O_4$–λ-MnO_2–$Li_4Mn_5O_{12}$ tie-triangle, and the 3 V region within the $LiMnO_2$–$LiMn_2O_4$–$Li_4Mn_5O_{12}$–Li_2MnO_3 tie-quadrilateral (Fig. 1b). Because the stoichiometric spinels $Li_{1+\delta}Mn_{2-\delta}O_4$ that are located on the tie-line between $LiMn_2O_4$ and $Li_4Mn_5O_{12}$ have lithium in both the tetrahedral A-sites and octahedral B-sites, it is possible that lithium extraction from these stoichiometric spinels can occur initially either at 3 V (if lithium is extracted from the octahedral sites) or at 4 V (if lithium is extracted from the tetrahedral sites). At the present time, there is insufficient structural and electrochemical data to define the exact line in the phase diagram that distinguishes the 4 V region from the 3 V region; from the data at hand, it is evident that this line lies fairly close to the $LiMn_2O_4$–$Li_4Mn_5O_{12}$ tie-line.

The onset of the Jahn–Teller distortion in lithiated-spinel electrodes occurs when the average oxidation state reaches approximately 3.5 [12]; it is represented by the broken line in Fig. 1b that is a tie-line of constant valence $n^+_{Mn} = 3.5$. It can therefore be understood from Fig. 1b that 4 V electrode materials that can discharge through the stoichiometric $LiMn_2O_4$–$Li_4Mn_5O_{12}$ tie-line into a cubic, 3 V region in which the Jahn–Teller distortion is suppressed (for example, those electrodes whose compositions pass through the shaded area in Fig. 1b) will be more stable to overdischarge than a $Li_xMn_2O_4$ electrode in which the Jahn–Teller effect occurs very close to the stoichiometric spinel composition ($x \approx 1.08$) [1].

3.1. Structural and electrochemical characterization of doped-spinel electrodes

3.1.1. Stoichiometric spinel electrodes, $Li_{1+\delta}Mn_{2-\delta}O_4$ ($0 \le \delta \le 0.33$)

Fig. 2 shows the powder X-ray diffraction patterns of stoichiometric $Li_{1+\delta}Mn_{2-\delta}O_4$ spinels synthesized during this study; the patterns could be indexed to the prototypic spinel space group Fd3m. Lattice constants and theoretical electrochemical parameters of the various phases are given in Table 1. The lattice constant decreases with x (Fig. 3). In spinel notation these stoichiometric compounds are represented by the formula $(Li)_{8a}[Mn_{2-\delta}Li_\delta]_{16d}O_4$. Therefore, as δ increases, the manganese ions in the octahedral (16d) sites are replaced by lithium ions with a concomitant increase in the manganese-ion oxidation state to maintain charge neutrality. The limiting composition $Li[Mn_{1.66}Li_{0.33}]O_4$ ($Li_4Mn_5O_{12}$) is reached when all the manganese ions are tetravalent.

The theoretical capacity that can be delivered at 4 V by the spinel electrode decreases with increasing δ. $LiMn_2O_4$ ($\delta = 0$) offers the highest 4 V capacity (154 mAh/g), based on the mass of the fully-oxidized composition Mn_2O_4 (Table 2), whereas an ideal $Li_4Mn_5O_{12}$ electrode ($\delta = 0.33$) offers no capacity at all at 4 V because the manganese ions are tetravalent (it is not possible to oxidize these cations further by electrochemical extraction of lithium, at least at practical voltages).

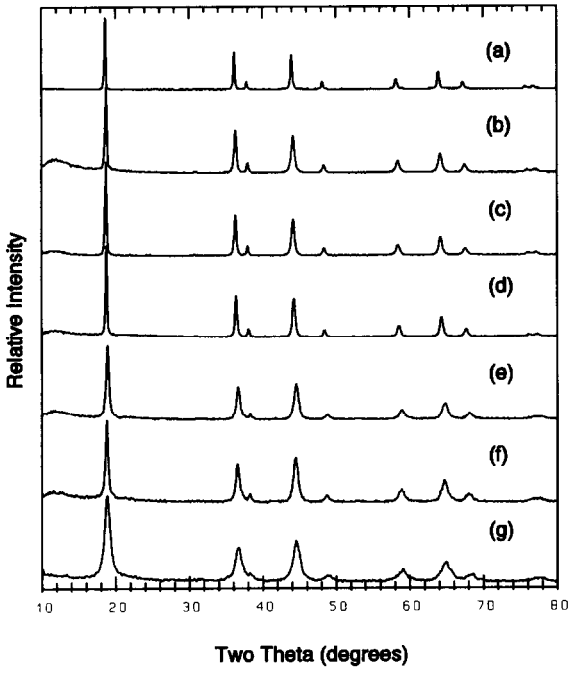

Fig. 2. Powder X-ray diffraction patterns of $Li_{1+\delta}Mn_{2-\delta}O_4$ spinels: (a) $\delta=0$, (b) $\delta=0.03$, (c) $\delta=0.05$, (d) $\delta=0.10$, (e) $\delta=0.22$, (f) $\delta=0.29$ and (g) $\delta=0.33$.

Figs. 4 and 5a–d show the cycling characteristics of four $Li/Li_{1+\delta}Mn_{2-\delta}O_4$ cells for the initial 10 charge/discharge cycles between 4.45 V and 3.50 V. The standard $Li/LiMn_2O_4$ cell initially delivers 118 mAh/g but loses capacity on cycling, albeit slowly (Figs. 4a, 5a). By contrast, the three lithium-doped spinels show a significantly enhanced cycling stability. However, this stability is gained at the expense of capacity. When $\delta=0.03$, an initial capacity of 101 mAh/g was achieved and when $\delta=0.10$ the initial capacity was 77 mAh/g. In these cells the discharge capacity was observed to increase marginally with cycling (Fig. 5b–d). The cycling stability of the lithium-doped spinels compared to the standard $LiMn_2O_4$ was attributed predominantly to the suppression of the Jahn–Teller distortion in the spinel electrode at the end of discharge.

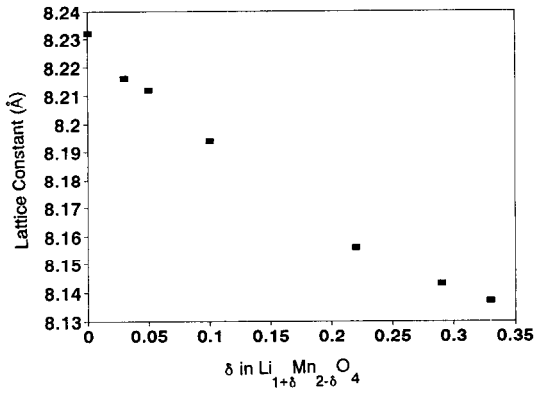

Fig. 3. A plot of lattice constant versus δ in $Li_{1+\delta}Mn_{2-\delta}O_4$ spinels.

Preliminary solubility data indicate that these

Table 1
Lattice constants and theoretical electrochemical parameters of various phases.

Stoichiometry of spinel phases $Li_{1+\delta}Mn_{2-\delta}O_4$	δ	Lattice constant (Å)	Theoretical Mn oxidation state	Fully oxidised composition	Theoretical capacity [a] (mAh/g)	n_{Li} [b]
$LiMn_2O_4$	0	8.232(1)	3.50	Mn_2O_4	154	0
$Li_{1.03}Mn_{1.97}O_4$	0.03	8.216(1)	3.54	$Li_{0.12}Mn_{1.97}O_4$	141	0.075
$Li_{1.05}Mn_{1.95}O_4$	0.05	8.212(1)	3.56	$Li_{0.20}Mn_{1.95}O_4$	132	0.125
$Li_{1.10}Mn_{1.90}O_4$	0.10	8.194(1)	3.63	$Li_{0.40}Mn_{1.9}O_4$	110	0.250
$Li_{1.22}Mn_{1.78}O_4$	0.22	8.156(2)	3.81	$Li_{0.88}Mn_{1.78}O_4$	54	0.550
$Li_{1.29}Mn_{1.71}O_4$	0.29	8.143(1)	3.92	$Li_{1.16}Mn_{1.71}O_4$	21	0.725
$Li_{1.33}Mn_{1.67}O_4$	0.33	8.137(1)	4.00	$Li_{1.33}Mn_{1.67}O_4$	0	0.825

[a] Theoretical capacity, based on the mass of the fully-oxidized composition, when discharged to the stoichiometric spinel composition, $Li_{1+\delta}Mn_{2-\delta}O_4$.

[b] The number of lithium ions that can be inserted into the stoichiometric spinel electrode before the onset of the Jahn–Teller distortion at $n^*_{Mn}=3.5$.

Table 2
Properties of $LiM_{\delta/2}Mn_{2-\delta}O_4$ spinel phases ($0 \leqslant \delta \leqslant 0.1$).

Stoichiometry of spinel phases $LiM_{\delta/2}Mn_{2-\delta}O_4$	δ	Experimetal lattice constant (Å)	Theoretical Mn oxidation state	Fully oxidised composition	Theoretical capacity [a] (mAh/g)
$LiMn_2O_4$	0	8.232(1)	3.50	Mn_2O_4	154
$LiMg_{0.025}Mn_{1.95}O_4$	0.05	8.218(1)	3.56	$Li_{0.15}Mg_{0.025}Mn_{1.95}O_4$	132
$LiZn_{0.025}Mn_{1.95}O_4$	0.05	8.224(3)	3.56	$Li_{0.15}Zn_{0.025}Mn_{1.95}O_4$	131
$LiMg_{0.05}Mn_{1.9}O_4$	0.10	8.202(1)	3.63	$Li_{0.3}Mg_{0.05}Mn_{1.90}O_4$	113

[a] Theoretical capacity, based on the mass of the fully-oxidised composition, when discharged to the composition, $LiMi_{d/2}Mn_{2-d}O_4$.

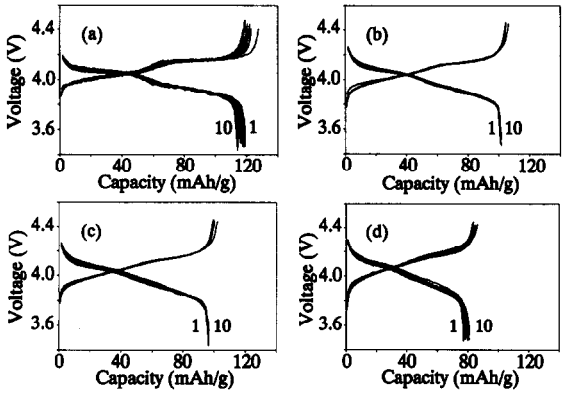

Fig. 4. Galvanostatic cycling data for the first 10 cycles of $Li/Li_{1+\delta}Mn_{2-\delta}O_4$ cells: (a) $\delta=0$, (b) $\delta=0.03$, (c) $\delta=0.05$ and (d) $\delta=0.10$. Cycling limits 3.5–4.45 V. Charge current 0.2 mA/cm^2, discharge current 0.4 mA/cm^2.

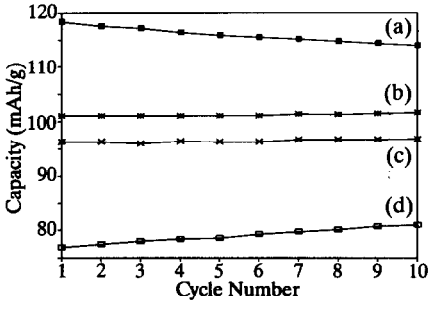

Fig. 5. Graph of discharge capacity versus cycle number for the first 10 cycles of $Li/Li_{1+\delta}Mn_{2-\delta}O_4$ cells shown in Fig. 4a–d: (a) $\delta=0$, (b) $\delta=0.03$, (c) $\delta=0.05$ and (d) $\delta=0.10$.

doped spinels which have a higher Mn^{4+} content than $LiMn_2O_4$ also suppress the disproportionation reaction

$$2Mn^{3+} \rightarrow Mn^{4+} + Mn^{2+}$$

thereby providing spinel electrodes with greater stability at 50–60°C. Further work, however, is necessary to confirm these preliminary data.

It should also be noted from Table 1 that the lattice constants of the doped-spinel phases are smaller than that of the standard $LiMn_2O_4$. Complete removal of lithium from $LiMn_2O_4$ in acid leaves λ-MnO_2 with $a=8.03$ Å [13]. By contrast, electrochemical removal of lithium from the doped-spinel phases leaves products with residual lithium that will restrict the lattice contraction. It is therefore anticipated that the unit-cell volume changes associated with lithium extraction/reinsertion reactions with doped-spinel phases at 4 V will be less than they are for $Li_xMn_2O_4$; this is an additional factor that is believed to promote structural stability of doped-spinel electrodes on cycling.

The data in Figs. 6 and 7a–b further emphasize the superior cycling ability of lithium-doped spinel electrodes over the standard $LiMn_2O_4$ electrode. In these experiments, a $Li/LiMn_2O_4$ cell (Figs. 6a, 7a) and a $Li/Li_{1.05}Mn_{1.95}O_4$ cell (Figs. 6b, 7b) were cycled galvanostatically between 2.70 and 4.45 V. The $Li/LiMn_2O_4$ cell loses capacity rapidly because it enters the tetragonal region of the phase diagram at the end of discharge at 4 V, whereas the $Li/Li_{1.05}Mn_{1.95}O_4$ cell, which remains within the cubic region of the phase diagram delivers a significantly improved stability on cycling (note that the onset of the Jahn–Teller effect

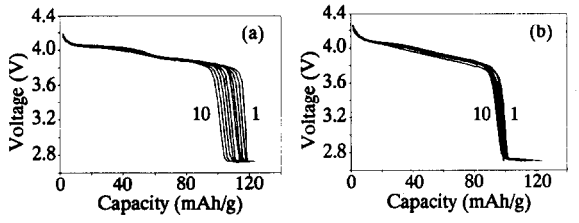

Fig. 6. Galvanostatic cycling data for the first 10 cycles of Li/$Li_{1+\delta}Mn_{2-\delta}O_4$ cells: (a) $\delta=0$, (b) $\delta=0.05$. Cycling limits 2.70–4.45 V. Charge current 0.2 mA/cm², discharge current 0.4 mA/cm².

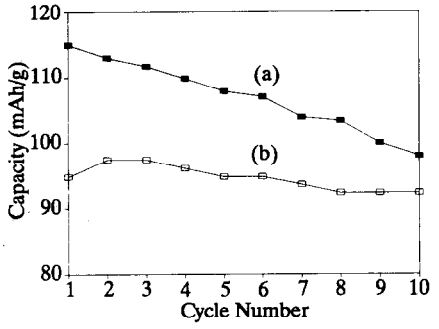

Fig. 7. Graph of discharge capacity above 3.5 V versus cycle number for the first 10 cycles of Li/$Li_{1+\delta}Mn_{2-\delta}O_4$ cells shown in Fig. 6a–b: (a) $\delta=0$, (b) $\delta==0.05$.

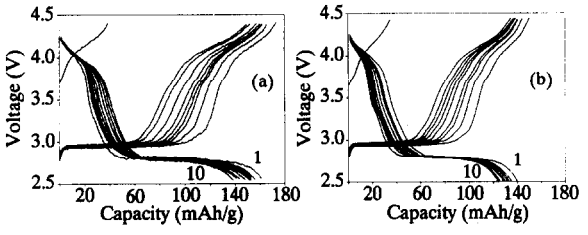

Fig. 8. Galvanostatic cycling data for the first 10 cycles of Li/$Li_{1+\delta}Mn_{2-\delta}O_4$ cells: (a) $\delta=0.22$, (b) $\delta=0.29$. Cycling limits 2.50–4.45 V. Charge current 0.2 mA/cm², discharge current 0.4 mA/cm².

in $Li_{1.05}Mn_{1.95}O_4$ should occur theoretically after 19 mAh/g has been delivered by the electrode in the 3 V region when it reaches the composition $Li_{1.175}Mn_{1.95}O_4$).

The cycling performance of Li/$Li_{1.22}Mn_{1.77}O_4$ ($\delta=0.22$) and Li/$Li_{1.29}Mn_{1.71}O_4$ ($\delta=0.29$) cells is given in Figs. 8a and 8b respectively. As expected, very little capacity can be drawn from these spinel electrodes at 4 V (Table 1). However, because the cubic symmetry of the $Li_{1.22+x}Mn_{1.77}O_4$ and $Li_{1.29+x}Mn_{1.71}O_4$ electrodes extends fairly deep into the cubic, 3 V region of the phase diagram, these cells show reasonably good reversibility when cycled over both the 3 V and 4 V regions; they yield total capacities of 160 mAh/g and 140 mAh/g on the initial discharge cycles, respectively. In principle, therefore, it should be possible to optimize the cycling efficiency of a high-capacity spinel electrode that operates at both 4 V and 3 V by careful selection of the initial spinel composition and by controlling the depth of discharge on the 3 V plateau.

3.1.2. $LiM_{\delta/2}Mn_{2-\delta}O_4$ (M=Mg, Zn) spinel electrodes

In principle, any monovalent or multivalent metal cation may be used instead of lithium to enhance the stability of lithium-manganese-oxide spinel electrodes. This principle was demonstrated by doping $LiMn_2O_4$ with Mg and Zn according to the general formula $LiM_{\delta/2}Mn_{2-\delta}O_4$, where M is a metal cation with oxidation state 2+. These doped-spinel phases

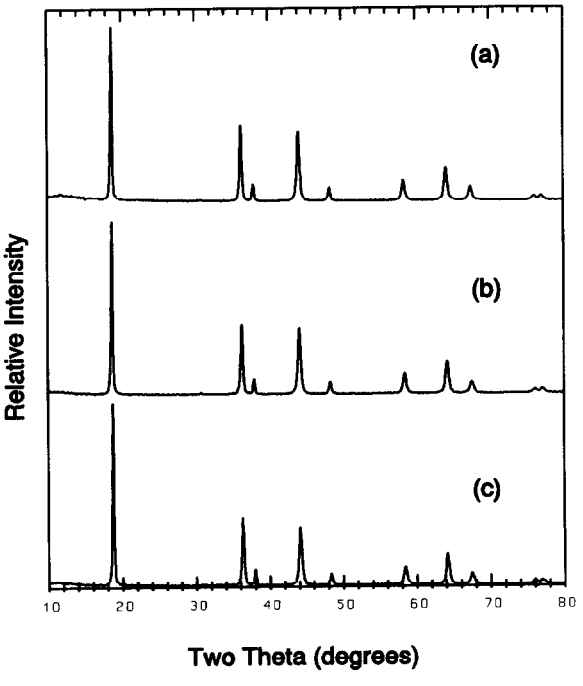

Fig. 9. Powder X-ray diffraction patterns of $LiM_{\delta/2}Mn_{2-\delta}O_4$ spinels: (a) M=Mg $\delta=0.05$, (b) M=Mg $\delta=0.10$ and (c) M=Zn $\delta=0.05$.

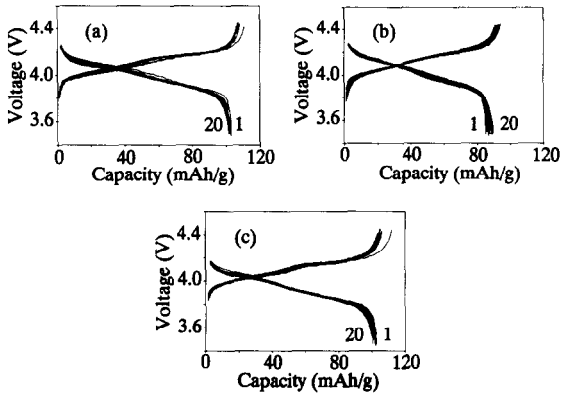

Fig. 10. Galvanostatic cycling data for the first 20 cycles of Li/$M_{\delta/2}Mn_{2-\delta}O_4$ cells: (a) M=Mg δ=0.05, (b) M=Mg δ=0.10 and (c) M=Zn δ=0.05. Cycling limits 3.50–4.45 V. Charge current 0.2 mA/cm^2, discharge current 0.4 mA/cm^2.

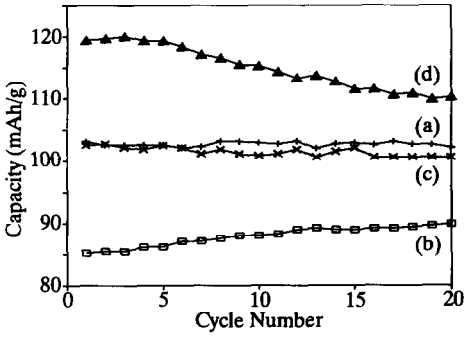

Fig. 11. Graph of discharge capacity versus cycle number for the first 20 cycles of Li/$M_{\delta/2}Mn_{2-\delta}O_4$ cells shown in Fig. 10 a–c: (a) M=Mg δ=0.05, (b) M=Mg δ=0.10 and (c) M=Zn δ=0.05.

are cation-deficient. Note, however, that stoichiometric spinels doped with a M cation can also be synthesized, for example $LiMg_{0.025}Mn_{1.975}O_4$ in which $n^+_{Mn}=3.52$, but that the cation-deficient spinels can accommodate more lithium.

The powder X-ray diffraction patterns of Mg- and Zn-doped spinels are shown in Fig. 9(a–c). Lattice constants of the various phases and theoretical electrochemical parameters are listed in Table 2. Cycling data of cells containing Mg-doped electrodes with δ=0.05 and δ=0.10 and Zn-doped electrodes with δ=0.05 are presented in Figs. 10 and 11. The data for a cell containing the standard spinel $LiMn_2O_4$ is shown in Fig. 11a for comparison. Excellent rechargeability was obtained from cells with a $LiMg_{0.025}Mn_{1.95}O_4$ electrode (103 mAh/g), a $LiZn_{0.025}Mn_{1.95}O_4$ (102 mAh/g) electrode and a $LiMg_{0.05}Mn_{1.90}O_4$ (90 mAh/g) for at least 20 cycles.

3.1.3. Defect spinels $Li_{1-\delta}Mn_{2-2\delta}O_4$ ($0<\delta\leq 0.11$)

Defect spinels with the general formula $Li_{1-\delta}Mn_{2-2\delta}O_4$ ($0<\delta\leq 0.11$) are located on the tie-line in the Li–Mn–O phase diagram between $LiMn_2O_4$ (δ=0) and $Li_{0.89}Mn_{1.78}O_4$ (δ=0.11, alternatively $Li_2Mn_4O_9$) (Fig. 1b). As δ increases, so does the number of vacancies in the structure and the average manganese-ion oxidation state. The limiting composition $Li_{0.89}Mn_{1.78}O_4$, in which all the manganese ions are tetravalent, has the cation distribution, in spinel notation, $(Li_{0.89}\square_{0.11})_{8a}[Mn_{1.78}\square_{0.22}]_{16d}O_4$, with vacancies on both the tetrahedral (8a) and octahedral (16d) sites [14].

Defect spinels with $0<\delta\leq 0.11$ can be formed by reaction of lithium and manganese salts (including hydroxides) at temperatures between 400°C and 600°C. In practice, however, they are difficult to prepare with a precise, predetermined composition; it is easier to prepare the stoichiometric spinel and extract the lithium in an electrochemical cell to reach the required composition. The powder X-ray diffraction pattern of a defect spinel with approximate composition $Li_{0.975}Mn_{1.95}O_4$ (δ=0.025) is shown in Fig. 12. Table 3 provides theoretical structural and electrochemical data that show the effect of δ on the average manganese oxidation state, the fully-oxidized composition and on the capacity that can be achieved at 4 V. In $Li_{0.975}Mn_{1.95}O_4$, the average manganese-ion oxidation state is 3.60; it has a lattice parameter of 8.218 Å which is slightly smaller than that of the standard $LiMn_2O_4$ electrode prepared for this investigation, 8.232 Å (Table 3). The initial capacity obtained from a Li/$Li_{0.975}Mn_{1.95}O_4$ cell was 117 mAh/g (Figs. 13, 14). However, the cycling stability was inferior to that obtained from cells with lithium-, magnesium- and zinc-doped spinel electrodes. Because $Li_{1-\delta}Mn_{2-2\delta}O_4$ defect spinels are difficult to prepare reproducibly as high-quality electrodes, it is probable that they will not be used as the initial electrodes in rechargeable lithium cells.

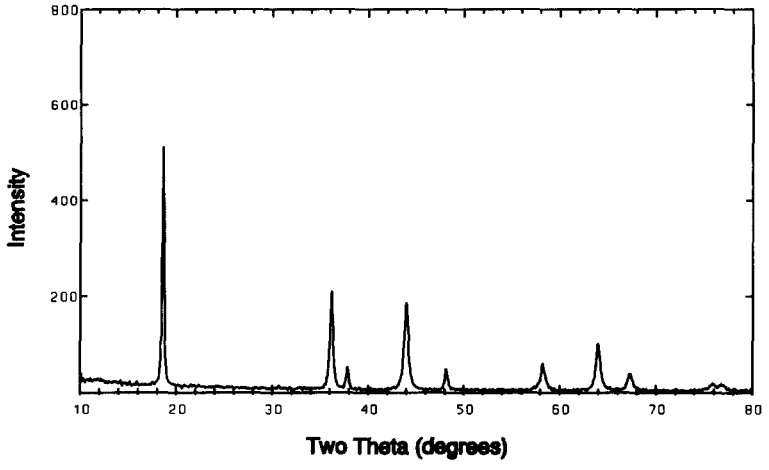

Fig. 12. Powder X-ray diffraction pattern of a $Li_{1-\delta}Mn_{2-2\delta}O_4$ cell ($\delta \approx 0.025$).

Table 3
Theoretical, structural and electrochemical data on the effect of δ on the average Mn oxidation state.

Stoichiometry of spinel phases $Li_{1-\delta}Mn_{2-2\delta}O_4$	δ	Experimental lattice constant (Å)	Theoretical Mn oxidation state	Fully oxidised composition	Theoretical capacity [a] (mAh/g)
$LiMn_2O_4$	0	8.232(1)	3.50	Mn_2O_4	154
$Li_{0.975}Mn_{1.95}O_4$	0.025	8.218(2)	3.60	$Li_{0.20}Mn_{1.95}O_4$	132
$Li_{0.95}Mn_{1.90}O_4$	0.050	–	3.70	$Li_{0.40}Mn_{1.90}O_4$	110
$Li_{0.89}Mn_{1.78}O_4$	0.11	8.174(1)	4.0	$Li_{0.89}Mn_{1.78}O_4$	0

[a] Theoretical capacity, based on the mass of the fully-oxidised composition, when discharged to the composition, $Li_{1-\delta}Mn_{2-2\delta}O_4$.

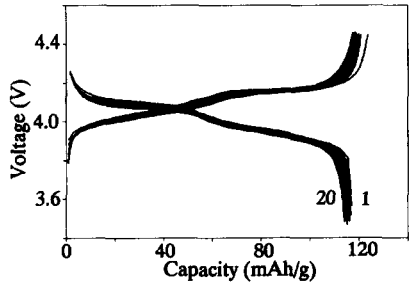

Fig. 13. Galvanostatic cycling data for the first 20 cycles of a Li/$Li_{1-\delta}Mn_{2-2\delta}O_4$ cell: Cycling limits 3.50–4.45 V. Charge current 0.2 mA/cm^2, discharge current 0.4 mA/cm^2.

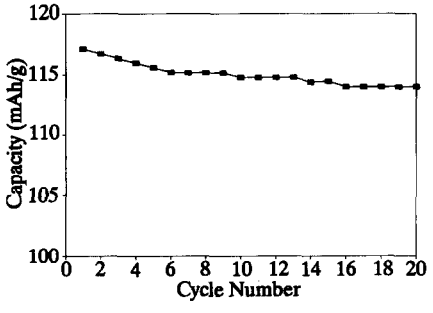

Fig. 14. Graph of discharge capacity versus cycle number for the first 20 cycles of the Li/$Li_{1-\delta}Mn_{2-2\delta}O_4$ cell shown in Fig. 13.

4. Conclusions

Improved capacity retention in rechargeable 4 V Li/$LiMn_2O_4$ cells has been demonstrated when a small amount of manganese in the spinel cathode is replaced with lithium, magnesium or zinc to increase the average manganese oxidation state in the initial electrode slightly above 3.5. The improved rechargeability, which is gained at the expense of capacity, is attributed primarily to the suppression of the Jahn–Teller effect on deep discharge of the doped-spinel cathodes. Furthermore, unlike $LiMn_2O_4$ that yields an unstable λ-MnO_2 electrode on complete extraction of lithium, all the lithium cannot be removed from doped-spinel structures; it is believed that the presence of this residual lithium in delithiated-spinel electrodes is also significant in enhancing their stability to repeated insertion/extraction of lithium. This work has demonstrated that it is possible to fabricate spinel electrodes that can deliver rechargeable capacities at 4 V in excess of 100 mAh/g for many cycles. Further work is still required to optimize the composition of spinel structures in order to enhance the capacity of these electrodes to render them attractive for commercial applications.

References

[1] M.M. Thackeray, W.I.F. David, P.G. Bruce and J.B. Goodenough, Mater. Res. Bull. 18 (1983) 461.
[2] M.M. Thackeray, P.J. Johnson, L.A. de Picciotto, P.G. Bruce and J.B. Goodenough, Mater. Res. Bull. 19 (1984) 179.
[3] D. Guyomard and J.M. Tarascon, J. Electrochem. Soc. 139 (1992) 937.
[4] A. Momchilov, V. Manev and A. Nassalevska, J. Power Sources 41 (1993) 305.
[5] J.M. Tarascon and D. Guyomard, Electrochim. Acta 38 (1993) 1221.
[6] T. Ohzuku, M. Kitagawa and T. Hirai, J. Electrochem. Soc. 137 (1990) 769.
[7] J.M. Tarascon, E. Wang, F.K. Shokoohi, W.R. McKinnon and S. Colson, J. Electrochem. Soc. 138 (1991) 2859.
[8] D. Guyomard and J.M. Tarascon, J. Electrochem. Soc. 140 (1993) 3071.
[9] R. Bittihn, R. Herr and D. Hoge, J. Power Sources 43–44 (1993) 223.
[10] Y. Toyoguchi, European Patent Application, No. 0 390 185 (1990).
[11] R.J. Gummow, PhD Thesis (University of Cape Town, 1993).
[12] M.M. Thackeray, A. de Kock, M.H. Rossouw, D.C. Liles, R. Bittihn and D. Hoge, J. Electrochem. Soc. 139 (1992) 364.
[13] J.C. Hunter, J. Solid State Chem. 39 (1981) 142.
[14] A. de Kock, M.H. Rossouw, L.A. de Picciotto, M.M. Thackeray, W.I.F. David and R.M. Ibberson, Mater. Res. Bull. 25 (1990) 657.